Journal of Catalysis **195,** 67–78 (2000)
doi:10.1006/jcat.2000.2969, available online at http://www.idealibrary.com on IDEAL®

Alumina-Supported Vanadium Oxide in the Dehydrogenation of Butanes

M. E. Harlin,*[,1] V. M. Niemi,† and A. O. I. Krause*

*Industrial Chemistry, Helsinki University of Technology, P.O. Box 6100, FIN-02015 HUT, Finland;
and †Fortum Oil and Gas Oy, P.O. Box 310, FIN-06101 Porvoo, Finland

Received March 3, 2000; revised May 25, 2000; accepted June 17, 2000

The activity of an alumina-supported vanadium oxide catalyst was studied in the dehydrogenation of *i*-butane and *n*-butane at 580°C under atmospheric pressure. The dehydrogenation reaction of the butanes to butenes and hydrogen was found to be catalysed by the reduced state of vanadium oxide (V^{4+} or V^{3+}, or possibly both). The activity of the catalyst was therefore studied in detail after reduction with H_2, CH_4, and CO. The activity was highest after CO reduction, even though the average oxidation states after the three reductions were similar. It was concluded that the main reason for the lower activity after H_2 and CH_4 reduction was the formation of OH groups that decreased the number of active sites for the dehydrogenation reaction. The primary cause of the catalyst deactivation during dehydrogenation was the formation of coke. © **2000 Academic Press**

Key Words: **dehydrogenation; oxidative dehydrogenation; *n*-butane; *i*-butane; vanadium oxide; catalysis.**

INTRODUCTION

Vanadium oxides have been extensively studied as catalysts in the oxidative dehydrogenation of light alkanes to alkenes and water (1–3). The oxidative dehydrogenation reaction is believed to proceed via the Mars–van Krevelen mechanism (4), in which the hydrocarbon reacts with lattice oxide ions leaving oxygen vacancies at the surface of the catalyst. In an oxidative atmosphere, the vacancies are then filled with oxygen from the gas phase, and the reduced cations are reoxidized.

Some studies on oxidative dehydrogenation have been carried out by using the pulse method without oxygen in the gas phase (5–8). Pantazidis *et al.* (5) studied a V–Mg–O catalyst in the oxidative dehydrogenation of propane. After 4500 pulses of propane, V^{5+} oxide was reduced to the oxidation state of V^{4+} or V^{3+}, and the conversion of propane obtained was 11% with a propene selectivity of 100%. Creaser *et al.* (6) recently reported that the vanadium oxide was reduced to oxidation state V^{2+} when propane was pulsed to V–Mg–O catalyst. In addition, Le Bars *et al.* (7) have reported for alumina-supported VO_x catalysts that even the lattice oxygen of γ-alumina may be consumed when the catalyst is reduced with ethane pulses, and the apparent oxidation state of vanadium may fall below zero. The oxygen balance is usually calculated according to the amounts of alkenes and CO_x that are formed and by assuming that the amount of water can be calculated from the stoichiometric reactions (6–8).

Alternatively, the activity of vanadium oxide catalysts has been related to the dehydrogenation of an alkane to the corresponding alkene and hydrogen (9–12). Vanadium oxide on alumina, silica, and aluminium phosphate supports was used in the dehydrogenation of propane, *n*-butane, and *i*-butane, but in none of these studies is there a detailed characterisation of the oxidation state of the vanadium oxide catalyst.

The reduction of vanadium oxide also has been widely studied. After calcination the vanadium oxide is mainly in oxidation state V^{5+}. On an alumina support it can be reduced to an average oxidation state between V^{4+} and V^{3+} by hydrogen, CO, and alkenes (13–16). The reduction behaviour of the calcined vanadium oxide is mainly influenced by the vanadium content of the catalyst and by the support (1, 16–18).

In unpublished work by Niemi (9), *n*-butane was reacted on an alumina-supported vanadium oxide (2.6–7.8 V atom/nm^2) catalyst at 580°C. The highest conversion of *n*-butane was obtained with vanadium loading between 2.6 and 5.2 V atom/nm^2. Above 5.2 V atom/nm^2 the conversion of *n*-butane decreased. Since the monolayer capacity of alumina is reported to be between 3.5 and 5.8 V atom/nm^2 (13, 17, 19–21), the decrease in activity above 5.2 V atom/nm^2 is likely due to the formation of crystalline V_2O_5.

One essential question in the dehydrogenation of alkanes with an oxide catalyst is whether the formation of alkenes takes place in reaction with catalyst oxygen or without the oxygen. In theory, resolving the question should not be difficult since water is formed among the products of oxidative dehydrogenation and hydrogen when oxygen is not reacting.

In an attempt to resolve this question, we studied the initial activity of vanadium oxide catalyst in the

---

[1] To whom correspondence should be addressed. Current address: Fortum Oil and Gas Oy. Fax: +358 10 45 27072. E-mail: elina.harlin@fortum.com.

0021-9517/00 $35.00

dehydrogenation of butanes, after calcination and after reduction of the catalyst with hydrogen, methane, and CO. Three reducing agents were used to evaluate the role of the reducing agent on the oxidation state of vanadium and on the activity of the catalyst. The reduction of the catalyst and the oxidation states present were characterised by temperature-programmed reduction and X-ray photoelectron spectroscopy. A vanadium content of 5% (3.3 V atom/nm^2) on alumina support was chosen for the study because, at this loading on alumina, the vanadium oxide should be well dispersed and, according to Niemi (9) and Clark *et al.* (10), the activity of the catalyst should be near its optimum in dehydrogenation.

EXPERIMENTAL

Catalyst Preparation

The vanadium oxide catalyst was prepared by incipient wetness impregnation on an alumina support. Prior to impregnation, the support (Akzo Nobel 000-1.5E) was crushed and sieved to a particle size of 0.3–0.5 mm and calcined at 750°C for 16 h with 5% oxygen in nitrogen (Aga, O_2 99.998%, N_2 99.999%).

The impregnation was accomplished by dissolving NH_4VO_3 (Merck, >99%) in an aqueous solution of oxalic acid (Riedel-de Haën AG, >99.5%). After impregnation the catalyst was dried at 120°C for 8 h and calcined at 700°C for 2 h.

Measurements of Catalyst Activity

The activity measurements were carried out at 580°C under atmospheric pressure in a fixed-bed microreactor. The catalyst was heated to the reaction temperature under 5% oxygen flow (Aga, O_2 99.5%, N_2 99.999%). The *n*-butane (Aga, 99.95%) or *i*-butane feed (Aga, 99.95%) with a weight hourly space velocity (WHSV) of 5 h^{-1} was diluted with nitrogen (Aga, 99.999%), the molar ratio of nitrogen to butane being 9 : 1. The nitrogen was purified with an Oxisorb (Messer Griesheim). The activity of the catalyst was followed for 15 min, after which the catalyst was flushed with nitrogen and regenerated with diluted air. Several cycles could be performed with the same catalyst. Before some of the activity measurements the catalysts were reduced with 5% hydrogen (Aga, 99.999%), 5% carbon monoxide (Messer Griesheim GmbH, 99.997%), or 10% methane (Merck, 99.995%) in nitrogen for 30 min at 585°C.

The products were analysed on-line with a Fourier transform infrared (FTIR) gas analyser (Gasmet, Temet Instruments Ltd.). The FTIR spectra were measured in the wavenumber range 850–4000 cm^{-1} with a resolution of 8 cm^{-1} at a scanning rate of 10 scans/s. The cuvette (9 cm^3) was maintained at constant temperature (175°C) and pressure (103 kPa). The method of analysing the reaction product by FTIR gas analysis has been discussed in detail elsewhere (22). During the first minute on stream, the spectra were measured every 3 s, they were then measured every 7 s, and after a few minutes every 30 s.

The conversion and selectivities were calculated from the reactor product on the basis of the carbon balance. The calculation is presented in detail elsewhere (23). If not otherwise stated, the coke formed on the catalyst during the dehydrogenation was not taken into account in the carbon balance.

Characterisation of the Catalysts

The amount of vanadium in the catalyst was measured by atomic absorption spectroscopy (AAS). The surface area of the catalyst was determined with a Coulter Omnisorp 100CX (static volumetric method). The crystalline structure was studied by X-ray diffraction (XRD) analysis with a Siemens D500 instrument using Cu$K\alpha$ radiation.

The reduction of the catalysts was studied by temperature-programmed reduction (H_2-TPR). The measurements were done with an Altamira Instruments AMI-100 catalyst characterisation system. Catalyst samples (50 mg) were dried at 130°C for 60 min with helium, calcined with 5% O_2/He at 600°C for 30 min, and cooled to 30°C in air. During the reduction the samples were heated from 30°C to 580°C at a rate of 5°C/min under 10% H_2 in argon (30 cm^3/min) and kept at the final temperature for 30 min. The consumption of hydrogen was measured with a thermal conductivity detector (TCD).

After temperature-programmed reduction to 580°C the catalyst was flushed with He (30 cm^3/min) for 15 min at 580°C. The catalyst was reoxidised at this temperature with 5% O_2/He (30 cm^3/min). The hydrogen retained on the surface of the catalyst during reduction was detected as outcoming water with a Balzers MSC 200 ThermoCube (MS) during oxidising treatment.

The oxidation states of vanadium oxide on the catalysts were investigated for selected samples by X-ray photoelectron spectroscopy (XPS). Before the measurements, the catalysts were heated to 580–585°C under 5% oxygen flow in the fixed-bed microreactor and some of the catalysts were then reduced with 5% H_2, 5% CO, or 10% CH_4 in N_2 for 30 min. After this, the catalysts were inertly transferred to a glove box and prepared for analysis under a nitrogen atmosphere. Finally they were transferred to the XPS instrument under vacuum.

The XPS measurements were performed in an X-probe model 101 spectrometer (Surface Science Instruments, VG Fisons) using a monochromatised Al$K\alpha$ X-ray source. A nickel grid and a flood gun were used to compensate the sample charging. The background pressure during acquisition was better than 1×10^{-6} Pa (1×10^{-8} Torr). High-resolution spectra of V 2*p*, Al 2*p*, O 1*s*, and C 1*s* and a low-resolution survey spectrum were measured using a nominal spot size of 600 μm. Atomic sensitivity factors provided by the instrument manufacturer were used to calculate the relative surface concentrations. The Al $2p$ line (74.5 eV) was used as a binding energy reference. The overlapping signals were deconvoluted using symmetrical Gaussian–Lorenzian (80/20) lines with the following constraints for all oxidation states: nonlinear Shirley background subtraction, an intensity ratio of V $2p_{3/2}$ to V $2p_{1/2}$ of 2.19, and a doublet separation (V $2p_{1/2} -$ V $2p_{3/2}$) of 7.3–7.6 eV.

RESULTS

Characterisation of the Fresh Vanadium Oxide Catalyst

The catalyst contained 5.2 wt% vanadium (AAS) and had a surface area of 165 m^2/g. After calcination at 750°C the surface area of the alumina support was 181 m^2/g.

The XRD pattern of the catalyst showed reflections only from the alumina support. The support was mostly γ-aluminium oxide, while some small peaks may indicate the presence of a minor amount of δ-aluminium oxide. Because the pattern of crystalline vanadium oxide was not detected, we assumed that the oxide was well dispersed on the surface of the support. Comparable results have been published by Koranne *et al.* (13) with a similar vanadium loading. The conclusion regarding the good dispersion of vanadium oxide was supported by the surface area measured for the catalyst and the H_2-TPR results presented below.

The XPS results are presented in Table 1 and in Fig. 1. After calcination at 582°C the vanadium oxide was totally in oxidation state 5+.

Catalytic Activity

The thermal reactions of butanes were studied in the absence of catalyst, with the catalyst replaced by carborundum of equal volume. Under the conditions used for the activity tests, the conversions of *i*-butane and *n*-butane were below 2%. With *i*-butane feed, the selectivity to *i*-butene was 54%, and with *n*-butane feed the selectivity to *n*-butenes (1-butene, *cis*-2-butene, *trans*-2-butene) and 1,3-butadiene was 41%.

TABLE 1

Results of Peak Deconvolution of the V Photoelectron Signal after Calcination of the Catalyst with Air and after Reduction with H_2, CH_4, or CO for 30 min at 580°C and Average Oxidation State Calculated from These Fractions

Treatment	V^{5+}	V^{4+}	V^{3+}	Average oxidation state of V
Calcination	100%, 517.6 eV	—	—	+5.0
H_2 reduction	21%, 517.5 eV	37%, 516.5 eV	42%, 515.9 eV	+3.8
CH_4 reduction	34%, 517.5 eV	28%, 516.5 eV	38%, 515.9 eV	+4.0
CO reduction	32%, 517.4 eV	41%, 516.4 eV	27%, 515.8 eV	+4.1

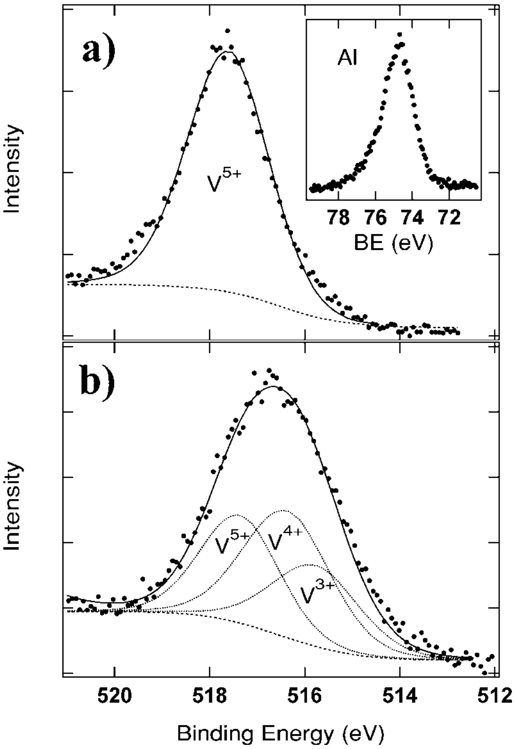

FIG. 1. Typical result of peak-fitting procedure for V $2p_{3/2}$ signal with (a) a calcined and (b) CO-reduced VO_x/Al_2O_3 catalyst. Measured signals are presented with dots. Inset: Al $2p$ line.

The activity of the calcined vanadium oxide catalyst was measured with *i*-butane feed at 580°C. The conversion of *i*-butane and the selectivities to *i*-butene and to *n*-butenes and 1,3-butadiene are presented in Fig. 2. The conversion of *i*-butane increased slightly from 22% at 1 min to 24% at 5 min. At the same time the selectivity to *i*-butene increased from 77% to 80%. The product distribution during the first 4 min on stream is presented in Fig. 3. Carbon oxides were the main products to form during the first minute on stream, probably due to the reduction of vanadium oxide by *i*-butane according to the following reaction:

$$C_4H_{10} + (4x+5)O^{2-} \rightarrow 4CO_x + 5H_2O + (8x+10)e^-. \quad [1]$$

However, the amount of water detected with the FTIR gas analyser (see Fig. 3) was substoichiometric relative to carbon oxides according to reaction [1]. The hydrocarbons were detected in the product stream about 10 s later than CO_x. The side reactions, cracking to methane and propene and isomerisation to *n*-butenes, may have been due to the acidic nature of the catalyst.

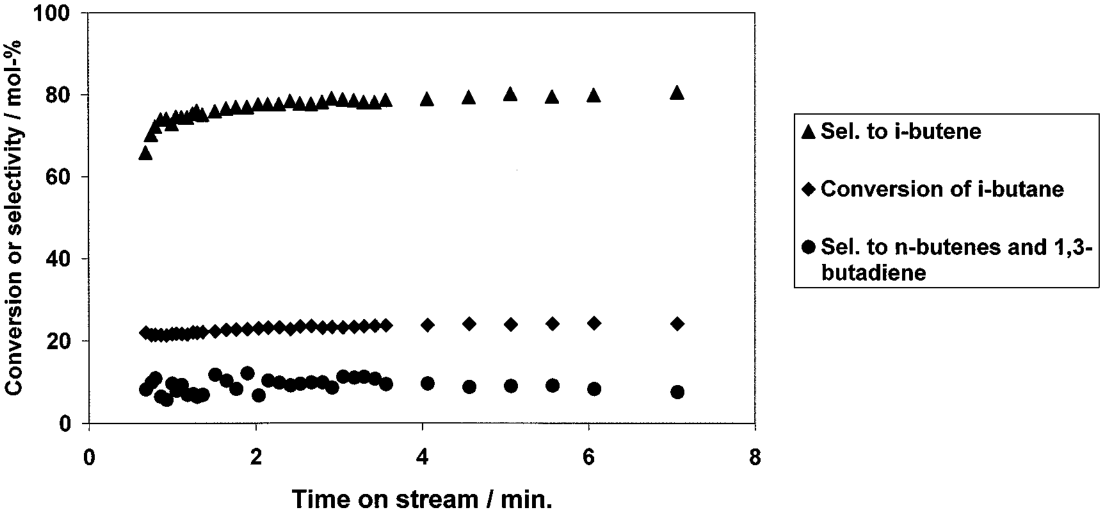

FIG. 2. Conversion of *i*-butane and selectivities with a calcined VO_x/Al_2O_3 catalyst.

The oxidation state of the vanadium oxide catalyst after calcination was 5+ (XPS). From the amount of carbon oxides measured by FTIR (Fig. 3) and the stoichiometric amount of water (reaction [1]), the molar ratio of the amount of released oxygen to vanadium (O/V) was calculated as 0.60 after 2 min on *i*-butane stream.

Under our conditions, i.e., without gas-phase oxygen, the formation of *i*-butene could be due to dehydrogenation (reaction [2]) or to oxidative dehydrogenation of *i*-butane (reaction [3]), as follows:

$$C_4H_{10} \rightleftharpoons C_4H_8 + H_2 \qquad [2]$$

$$C_4H_{10} + O^{2-} \rightarrow C_4H_8 + H_2O + 2e^-. \qquad [3]$$

If *i*-butene was formed according to reaction [3], vanadium oxide would at the same time be reduced to lower oxidation state. Because the amount of water detected in the product was lower than the stoichiometric amount of carbon oxides (reaction [1]), the existence of an oxidative dehydrogenation reaction cannot be deduced from the formation of water.

The conversion of *n*-butane and selectivities for the calcined vanadium oxide catalyst are shown in Fig. 4. The conversion of *n*-butane increased from 18% at 1 min to 23% at 5 min. The dehydrogenated products that formed were *n*-butenes and 1,3-butadiene. The 1-butene : *cis*-2-butene : *trans*-2-butene ratio of 1.1 : 1.0 : 1.1 observed from 0.7 min on stream onward is similar to the alkene distribution at thermodynamic equilibrium. A similarity with the equilibrium distribution is usual for acidic catalysts (1). During the first 0.7 min on stream the fraction of 1-butene was lower and the fraction of 1,3-butadiene higher.

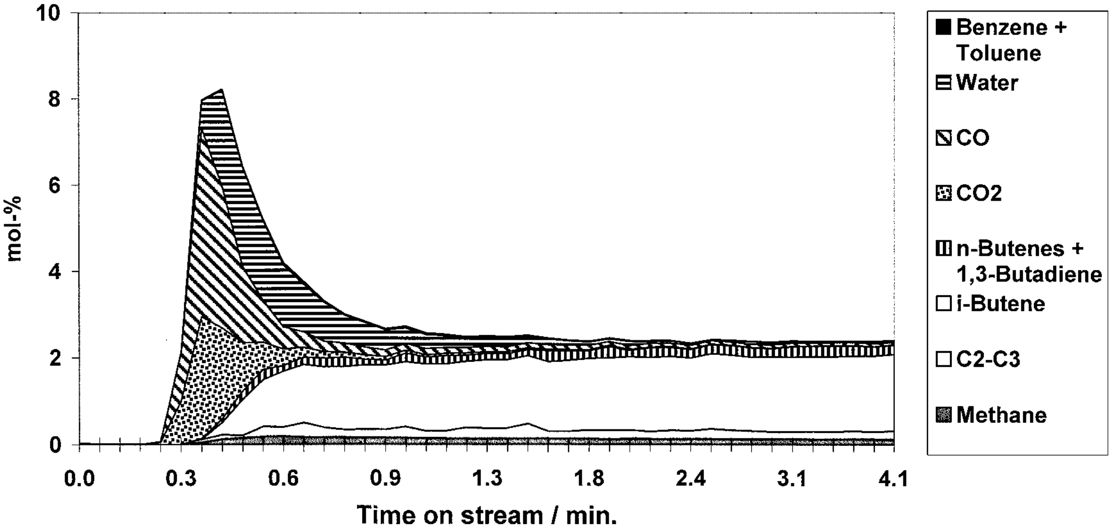

FIG. 3. Product distribution during the first 4 min on *i*-butane stream with a calcined VO_x/Al_2O_3 catalyst.

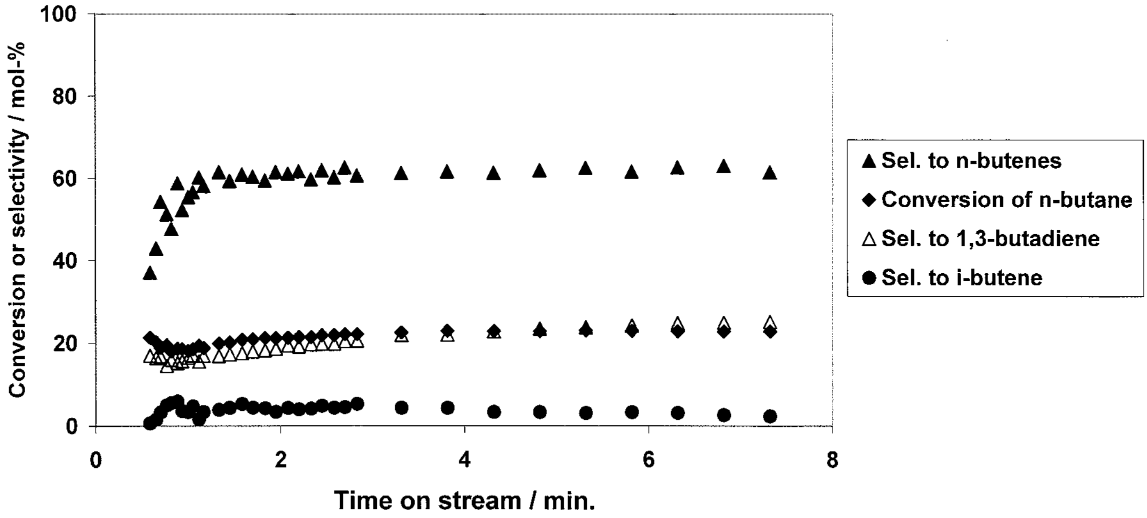

FIG. 4. Conversion of *n*-butane and selectivities with a calcined VO_x/Al_2O_3 catalyst.

1,3-Butadiene can be formed both by dehydrogenation of *n*-butenes and by oxidative dehydrogenation of *n*-butane and *n*-butenes (24). The ratio of 1,3-butadiene to *n*-butenes is presented in Fig. 5. From the amount of carbon oxides formed and the stoichiometric amount of water (reaction [1]), the molar ratio of O/V was calculated as 0.63 after 2 min on *n*-butane stream.

It is also possible, as reported by Pantazidis *et al.* (5) and Blasco *et al.* (24), that an alkane first reacts through oxidative dehydrogenation to alkenes and that these alkenes reduce vanadium oxide to a lower oxidation state. In this case the overall reaction would be similar to Eq. [1].

The dehydrogenation reaction [2] is limited by the thermodynamic equilibrium. At 580°C and 1 bar with an *i*-butane/nitrogen feed of 1 : 9 mol/mol, the equilibrium conversion of *i*-butane to *i*-butene is 89%. Under the same conditions with an *n*-butane/nitrogen feed of 1 : 9 mol/mol, the conversion of *n*-butane to 1-butene, *cis*-2-butene, *trans*-2-butene, and 1,3-butadiene is 88%. There are no thermodynamic limitations in reaction [3].

As presented above, several reactions are possible on the calcined vanadium oxide catalyst. As a next step we therefore used hydrogen, methane, and carbon monoxide to reduce vanadium to a lower oxidation state before the

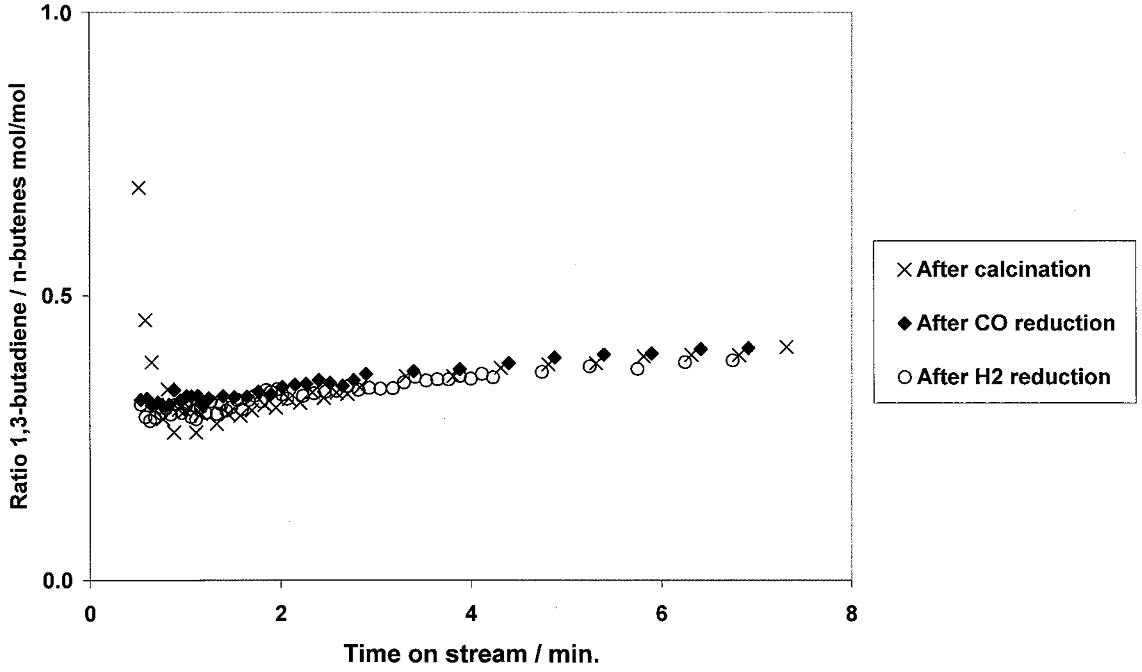

FIG. 5. Molar ratio of 1,3-butadiene to *n*-butenes formed with *n*-butane feed and a calcined, CO-reduced, and H_2-reduced VO_x/Al_2O_3 catalyst.

dehydrogenation. Three reducing agents were tested to explore the role of the oxidation state of vanadium in the dehydrogenation of butanes.

Reduction with H_2

The vanadium oxide catalyst was reduced with 5% hydrogen in nitrogen for 30 min as follows:

$$H_2 + O^{2-} \rightarrow H_2O + 2e^-. \quad [4]$$

During the reduction the amount of water measured by FTIR was 6.2×10^{-4} mol/g. This value leads to the molar ratio O/V of 0.61. It is possible, however, that part of the water formed during the H_2 reduction was retained on the surface and was not detected at the outlet of the reactor.

After the prereduction with hydrogen, the activity of the catalyst was measured with *i*-butane feed. The conversion of *i*-butane was 35% after 1 min on stream and the selectivity to *i*-butene 67%. After 5 min on stream the corresponding values were 32% and 79%. The results are presented in Fig. 6a. The amount of oxygen-containing species was low during the *i*-butane test: the molar ratio of O/V was just 0.01 during the first 2 min on stream.

Reduction with CH_4

Vanadium oxide was also reduced to its lower oxidation state with methane. The products formed were carbon oxides and water.

$$CH_4 + (x+2)O^{2-} \rightarrow CO_x + 2H_2O + (2x+4)e^-. \quad [5]$$

The consumption of methane during the reduction was estimated from the formation of carbon oxides according to reaction [5]. The value obtained for the molar ratio of O/V was 0.67. The amount of carbonaceous residues formed on the surface was about 0.8×10^{-4} mol/g, measured as the formation of carbon oxides during the following regeneration with air.

The activity of the catalyst measured with *i*-butane feed after methane reduction is shown in Fig. 6b. The conversion of *i*-butane was 41% and the selectivity to *i*-butene 72% after 1 min on stream, and the corresponding values were 35% and 82% after 5 min on stream. The formation of oxygen-containing species was low during the *i*-butane feed, the ratio of O/V being 0.02 (2 min).

Reduction with CO

The vanadium oxide was reduced with 5% carbon monoxide in nitrogen for 30 min according to the reaction

$$CO + O^{2-} \rightarrow CO_2 + 2e^-. \quad [6]$$

The amount of CO_2 measured by FTIR at the outlet of the reactor was 7.3×10^{-4} mol/g.

Carbon monoxide can also react according to the Boudouard reaction and form CO_2 and carbon:

$$2CO \rightleftharpoons CO_2 + C. \quad [7]$$

The amount of carbon formed during the reduction with CO was about 2.3×10^{-4} mol/g. On the assumption that the amount of CO_2 formed in reaction [7] is equal to the amount of carbon, we obtained 5.0×10^{-4} mol/g as the amount of CO_2 formed in reaction [6]. This yields a molar ratio of O/V 0.49 during the reduction with CO.

The results obtained with *i*-butane feed after carbon monoxide reduction are presented in Fig. 6c. After 1 min on *i*-butane stream the conversion of *i*-butane was 54% and the selectivity to *i*-butene 75%, and after 5 min on stream the corresponding values were 42% and 86%. The product distribution obtained during *i*-butane feed after CO reduction is presented in Fig. 7. As can be seen, the amount of oxygen-containing products released from the catalyst was very low (O/V 0.01 mol/mol).

Figures 6a–6c show that the highest activity in the *i*-butane dehydrogenation was obtained after the CO reduction. A more detailed study was therefore made of the catalyst after CO reduction to evaluate the reason for the higher activity.

After the CO reduction the catalyst was flushed with nitrogen and reduced again with 5% hydrogen in nitrogen for 5 min. The activity of the catalyst in *i*-butane dehydrogenation after these two reductions is presented in Fig. 8. It is seen that the conversion of *i*-butane and the selectivity to *i*-butene were the same as those after CO reduction.

The product formed during H_2 reduction of the calcined catalyst was water, and its effect on the activity was studied next. The catalyst was reduced with CO and, after initial flushing with nitrogen, 2% water was added to the nitrogen feed with a saturator for 3 min. After 2 min on a H_2O/N_2 stream, a water content of 2% was measured in the reactor effluent. The catalyst was again flushed with nitrogen, and the activity was measured with *i*-butane feed. The conversion of *i*-butane clearly decreased after the water treatment (Fig. 8). Evidently, however, the water treatment did not affect the oxidation state of the catalyst since the formation of oxygen-containing products was very low (O/V 0.04).

Activity with n-Butane Feed

The catalyst was also tested with *n*-butane feed, after reduction with CO or H_2. The results showed trends similar to those found with *i*-butane feed. The conversion of *n*-butane was higher after CO reduction, being 45% after 1 min on stream, and the selectivity to *n*-butenes and 1,3-butadiene was 83%. The corresponding values after H_2 reduction were 37% and 79%. The *n*-butene distribution of 1.1 : 1.0 : 1.1 (1-butene : *cis*-2-butene : *trans*-2-butene) was observed after reduction with CO and H_2. The molar ratios

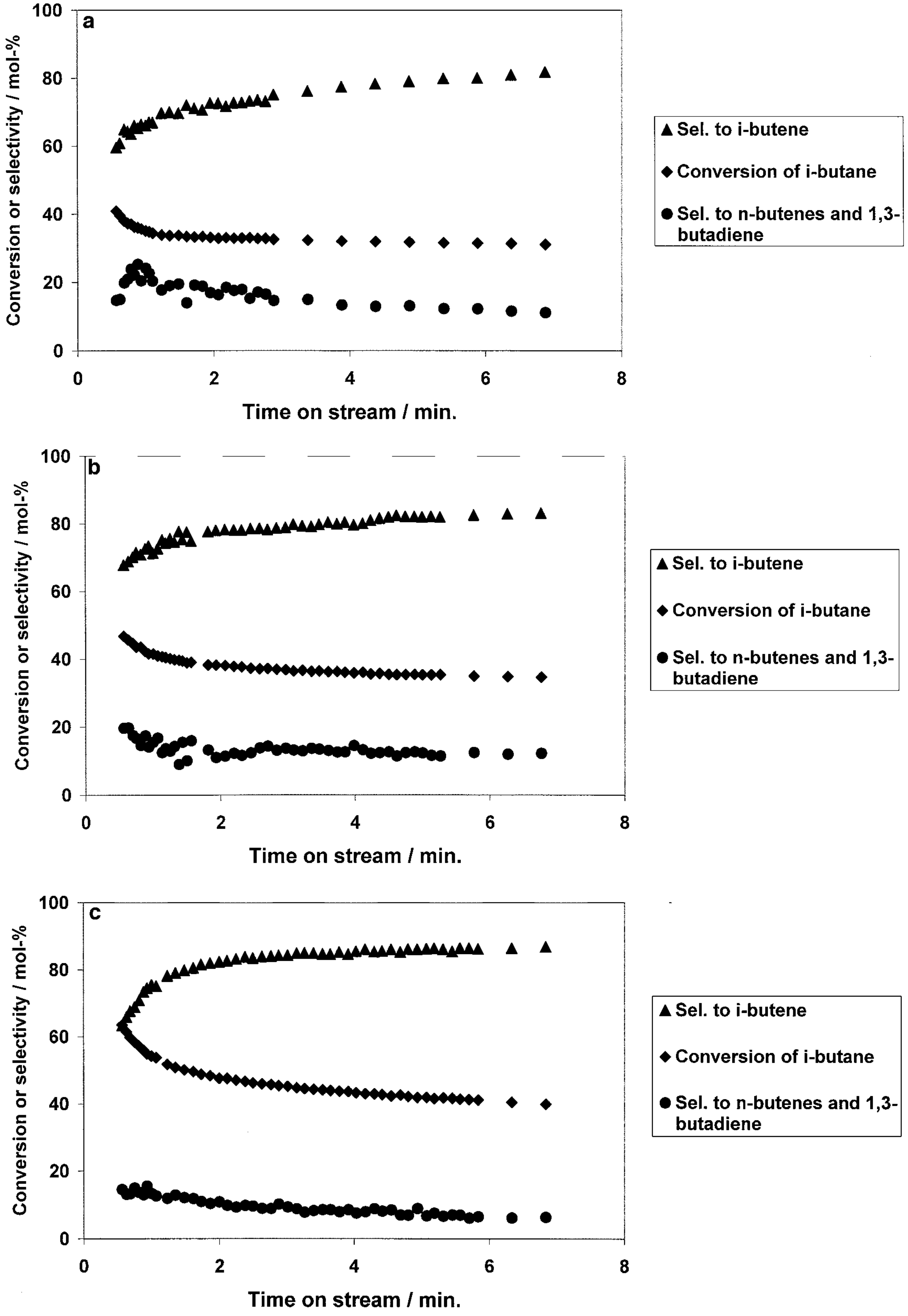

FIG. 6. Conversion of *i*-butane and selectivities (a) after H_2 reduction, (b) after CH_4 reduction, and (c) after CO reduction.

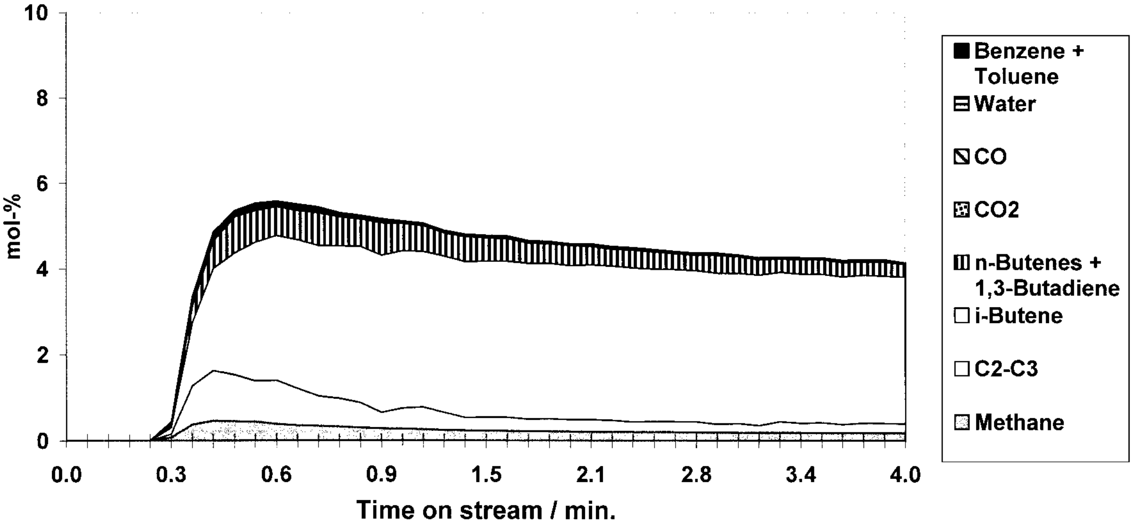

FIG. 7. Product distribution during the first 4 min on *i*-butane stream after CO reduction.

of 1,3-butadiene to *n*-butenes in the product stream are presented in Fig. 5.

Coke Formation

The results presented in Figs. 2, 4, and 6 do not take into account the formation of coke on the catalyst during the dehydrogenation. The amount of coke formed on the catalyst can be determined by measuring the amount of carbon oxides formed during the following regeneration (Table 2). The formation of coke can then be included in the calculation of conversion and selectivity. The amount of hydrocarbons formed is calculated for the whole 15 min period of the test and the amount of coke is added to the carbon balance. The results, including the formation of coke, are presented in Table 2 as an average for each test.

The average values shown in Table 2 describe well the activity of the catalyst when the conversion of butanes was stable as it was after calcination and after H_2 reduction. After CO reduction, however, the conversion decreased sharply. It is possible, therefore, that also the coke formation on the surface was not stable during the 15 min test. This possibility was studied by reducing the catalyst with CO for 30 min and then treating the catalyst with *i*-butane for 2, 6, or 15 min. The coke formation and the conversion of *i*-butane are presented in Fig. 9. The formation of coke was highest during the first 2 min on stream, and after that declined to a more or less stable level.

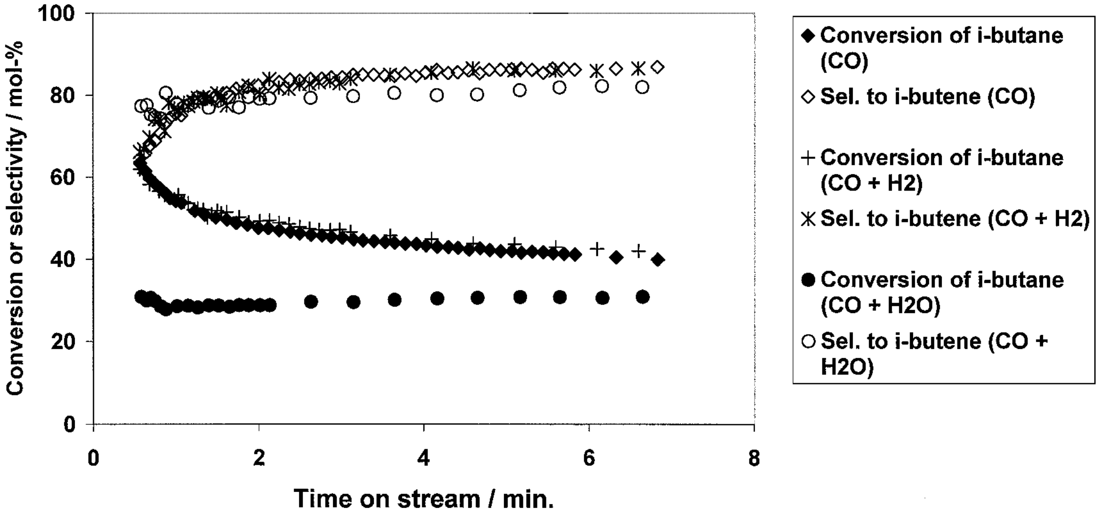

FIG. 8. Conversion of *i*-butane and selectivity to *i*-butene (◆, ◇) after CO reduction, (+, ⁎) after CO and H_2 reduction, and (●, ○) after CO reduction and H_2O treatment.

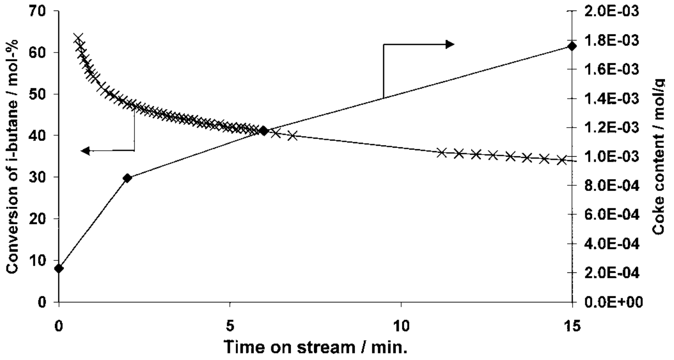

FIG. 9. Conversion of *i*-butane and the amount of coke formed on the catalyst. The VO_x/Al_2O_3 catalyst was prereduced with CO.

Oxidation States of Vanadium Oxide after Reduction

The catalysts were studied by XPS after reduction with hydrogen, methane, and carbon monoxide at 580–585°C. The results are presented in Table 1 and the peak deconvolution is illustrated in Fig. 1b. After the reductions, oxidation states of 5+, 4+, and 3+ were observed for vanadium. The fractions presented in Table 1 were calculated from the line V $2p_{3/2}$. Relative to the catalyst after the calcination, the change in the XPS V/Al ratio was −35% after H_2, −22% after CO, and −17% after methane reduction.

The reduction of vanadium oxide catalyst was also studied by H_2-TPR. The shape of the TPR profile (Fig. 10) indicated the presence of at least two maxima between 400 and 500°C, and a shoulder at 550°C. When the reduction was performed to 580°C, the consumption of hydrogen was 7.6×10^{-4} mol/g, corresponding to a molar ratio of H_2/V 0.75. Assuming a reduction stoichiometry of 0.5 H_2/V from V^{5+} to V^{4+}, the average oxidation state of vanadium would be 3.5+. After the reduction with hydrogen, the catalyst was flushed with He and treated with oxygen at 580°C. The water formation during the oxygen treatment was measured by MS. The amount of water was 1.1×10^{-4} mol/g, corresponding to a molar ratio H_2/V of 0.10.

Table 3 shows the average oxidation states of vanadium oxide after reduction with hydrogen, methane, and CO. The techniques used in the investigation were FTIR, XPS, and H_2-TPR. In one instance (FTIR) the water retainment of 0.10 (O/V) was taken into account in calculating the average oxidation state after H_2 reduction. As can be seen, the average oxidation states obtained with the three techniques and the three reducing agents were closely similar. However, the activities of the catalysts were different after

TABLE 2

Carbon Content after Dehydrogenation of *n*-Butane and *i*-Butane for 15 min and the Average Activities and Selectivities during 15 min When the Carbon Content Is Included in the Carbon Balance

Feed/ pretreatment	Coke (mol/g)	Conversion (%)	Selectivity to alkenes (%)[a]	Selectivity to coke (%)
n-Butane/ calcination	12.6×10^{-4}	22	78	7
i-Butane/ calcination	9.3×10^{-4}	24	76	5
i-Butane/ H_2 reduction	10.7×10^{-4}	32	77	4
i-Butane/ CH_4 reduction	12.5×10^{-4}	36	78	4
i-Butane/ CO reduction	17.6×10^{-4}	41	81	5

[a] *i*-Butene with *i*-butane feed and *n*-butenes and 1,3-butadiene with *n*-butane feed.

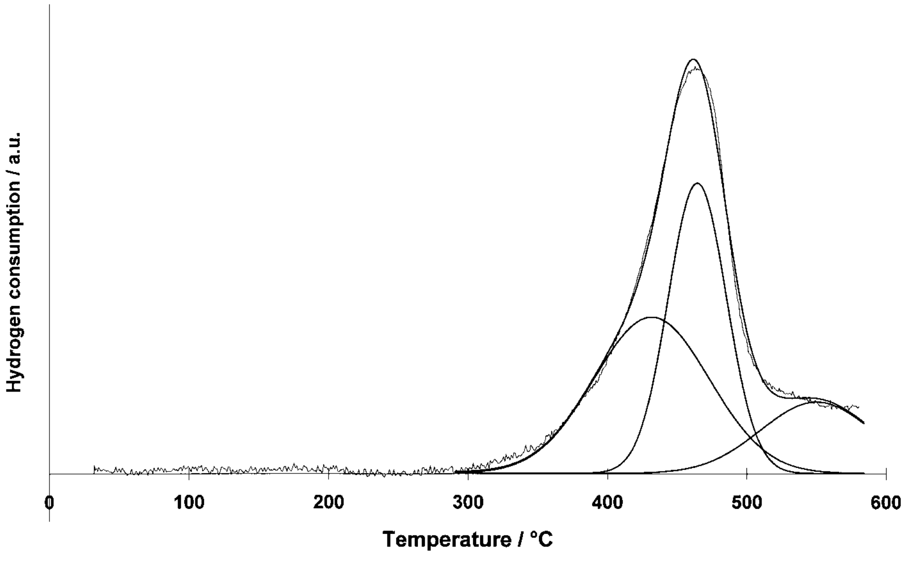

FIG. 10. H_2-TPR profile of the VO_x/Al_2O_3 catalyst.

TABLE 3

Average Oxidation State of Vanadium Oxide after Reduction with H_2, CH_4, and CO

	Average oxidation state of V		
	FTIR	XPS	H_2-TPR
Reduction with H_2	3.6	3.8	3.5
Reduction with CH_4	3.7	4.0	
Reduction with CO	4.0	4.1	

the three prereductions, as presented in Fig. 6. The conversion of *i*-butane was highest after reduction with CO, and lowest after reduction with H_2.

DISCUSSION

The conversion of *i*-butane and *n*-butane increased during dehydrogenation for 15 min with the calcined vanadium oxide catalyst. The product distribution measured on-line with the FTIR gas analyser showed that carbon oxides and water were released along with the increase in activity. However, the amount of water was substoichiometric compared to carbon oxides according to the reactions of butanes to carbon oxides and water. This means that the oxygen balance measured by FTIR could not be used to demonstrate whether butenes were formed in the reaction with catalyst oxygen. The MS measurement after H_2-TPR revealed that part of the water formed during reduction of vanadium oxide was adsorbed on the surface of the catalyst.

In the absence of gas-phase oxygen the reaction of butanes on calcined vanadium species can proceed through two parallel reactions: combustion of butane to CO_x and water and oxidative dehydrogenation to butenes and water. It is possible that the oxidative dehydrogenation required a partly reduced vanadium oxide catalyst and therefore began a few seconds later than combustion. However, both reactions proceeded until vanadium species were reduced to more or less stable oxidation states. According to the CO_x formation during butane dehydrogenation, the combustion resulted in a molar ratio of O/V of 0.6. By estimating the maximum extent of the reduction of VO_x to be 0.75 (Table 3), we see that the vanadium oxide catalyst was mainly reduced by combustion of butane to CO_x and water, while oxidative dehydrogenation was only a minor reaction. The change in the distribution of *n*-butenes and 1,3-butadiene detected on calcined vanadium oxide catalyst during the first minute on *n*-butane stream may have been due to a change from the oxidative dehydrogenation reaction to the dehydrogenation reaction (7).

Reduction with hydrogen, methane, and CO clearly increased the activity of the catalyst. The facts that vanadium oxide had been reduced to lower oxidation state before the test and no water was formed during *i*-butane feed after CO reduction (Fig. 7) argued strongly for the conclusion that the reaction was dehydrogenation and not an oxidative dehydrogenation reaction. The *i*-butene yield was so high that at least some water formation should have been observed with the FTIR gas analyser if the reaction had been oxidative dehydrogenation. This result led us to believe that the activity of the vanadium oxide catalyst in dehydrogenation might be related to the reduced valence state of vanadium.

Many factors may affect the activity of the catalyst in the dehydrogenation of butanes. We now discuss some of these factors, on the basis of the results obtained during this study.

Reduction and Oxidation States

The H_2-TPR pattern in Fig. 10 resembles that presented by Koranne *et al.* (13) for a similar vanadium loading. They proposed that the hydrogen consumption between 400 and 500°C is related to the reduction of the surface vanadium species. The bulk-like vanadium oxide was reduced at 640°C on alumina. Koranne *et al.* (13) proposed that, during the temperature-programmed reduction, the reduction of V^{5+} to V^{4+} corresponds to a consumption of 0.5 H_2/V. Haber *et al.* (16) found, in turn, that the reduction of V^{5+} to V^{4+} corresponds to a consumption of 0.75 H_2/V. The difference is based on their assumption of H_2 chemisorption and the formation of OH groups. Our results indicate a retainment of 0.1 H_2/V during the reduction to 580°C. On the basis of our previous studies (23, 25), where combinations of different characterisation techniques (XPS, FTIR, H_2-TPR) were applied during and after reductions, it seems likely that the hydrogen consumption measured with the TCD detector during the H_2-TPR study directly describes the change in the oxidation state of the catalyst. This means that, in this study, the water retained should be added to the water formed during H_2 reduction measured with the FTIR gas analyser, as has been done with the value presented in Table 3. The amount of water retained on the surface of the alumina-supported vanadium oxide is nevertheless minor at high temperatures. Therefore, despite the different conclusions about water retainment in the literature, the average oxidation state reported for vanadium after reduction with H_2 or CO has typically been between 3 and 4 (13, 15).

The oxidation states found in the reduced catalysts by XPS were V^{5+}, V^{4+}, and V^{3+}. Eberhardt *et al.* (15) only discovered the oxidation states V^{5+} and V^{3+} on the surface after reduction with H_2 or CO. It has often been concluded, however, that the alumina support stabilises the formation of V^{4+} species during reduction (13, 16, 26), and V^{4+} species have been measured on alumina by UV–visible and ESR spectroscopies by several authors (14, 21, 27, 28).

The fractions of the oxidation states V^{5+}, V^{4+}, and V^{3+} observed by XPS were slightly different after reductions with H_2, CH_4, and CO. However, no further reduction of the vanadium oxide was observed during a subsequent dehydrogenation test with *i*-butane. The activity of the catalyst was about the same after combined CO and hydrogen reduction as after CO reduction alone. This indicates that the oxidation states of vanadium were about the same after the different prereductions. Haber *et al.* (16) have similarly reported that the degree of reduction of the vanadium oxide is independent of the reducing agent (H_2, CO, or propane) between 400 and 600°C. The difference in the activities in the dehydrogenation of *i*-butane and of *n*-butane after the three prereductions must therefore be due to some other factor than the oxidation state of vanadium.

Dispersion of Vanadium Oxide

According to the XPS results, the molar ratio of vanadium to aluminium decreased during all three reductions. This ratio may be related to the decreased dispersion of vanadium oxide (8, 15). The lowest ratio was observed after reduction with hydrogen, and the dehydrogenation activity was also lowest with this catalyst. Perhaps, then, the differences between the activities in dehydrogenation after CO and H_2 reduction are, at least in part, related to differences in the number of active sites.

Water Retainment

Water retainment on the catalyst surface was observed during reduction with hydrogen, methane, and butanes. The amount of water, measured with a MS after H_2-TPR measurement (1.1×10^{-4} mol/g), was 0.13 mol/mol expressed as a molar ratio of water to the hydrogen consumption during the H_2-TPR measurement between 30 and 580°C. The results, presented in Fig. 8, clearly indicate that the water adsorbed on the catalyst surface before the dehydrogenation test decreased the activity of the catalyst. The inhibiting effect of water has also been observed by Oyama *et al.* (29) and Chen *et al.* (30). Oyama *et al.* (29) studied the effect of the partial pressure of water in ethane oxidation with V_2O_5/SiO_2 catalyst at 568°C, proposing that water adsorbs competitively on the surface, producing HO^* and leaving fewer O^* sites available for ethane adsorption. Chen *et al.* (30) suggested that the OH groups formed in the oxidative dehydrogenation of propane with VO_x/ZrO_2 catalyst recombine to form water reversibly; i.e., the water can dissociatively adsorb on the surface of the catalyst. The results of our present study support the conclusion that water was adsorbed on the catalyst surface at vacancies associated with either V^{3+} or V^{4+}, which form the active centres for dehydrogenation.

Carbonaceous Residues

It has often been discussed whether the coke formed on the catalyst surface has some influence on the activity of the catalyst (31). In the reduction treatments before the activity test, the amount of carbonaceous residues formed decreased in the order CO reduction (2.3×10^{-4} mol/g), methane reduction (0.8×10^{-4} mol/g), H_2 reduction (no coke formation). If carbon-containing vanadium species were the main reason for the dehydrogenation activity, the activity should have increased markedly during reduction with *n*-butane, to the same level as that after CO reduction, but this was not the case. Carbonaceous residues formed on the surface may still partly modify the activity. For example, the higher selectivity for dehydrogenation at the higher conversion level obtained after the CO reduction, compared with the results obtained after the H_2 reduction, may have been due to the greater amount of coke on the surface. The increase in selectivity during the butane tests was also likely due to the formation of coke on the surface.

CONCLUSIONS

The vanadium oxide catalyst was tested in the dehydrogenation of *n*-butane and *i*-butane at 580°C under atmospheric pressure. The activity of the catalyst was related to the reduced valence state of vanadium, either V^{4+} or V^{3+}, or possibly both. These species were formed during reduction of the catalyst with all reducing agents: butane, CO, methane, and H_2. The activity of the catalyst was highest after reduction with CO. The initial conversions of *i*-butane and *n*-butane were 64% and 55%, which are 72% and 63%, respectively, of the thermodynamic equilibrium values. The activity was lower after reduction with H_2, CH_4, and butane, possibly due to OH groups formed during these reductions and adsorbed on some of the reduced vanadium centres that are active in dehydrogenation. The low activity obtained after CO reduction and subsequent water treatment supports this suggestion. The decrease in activity and the increase in selectivity during the dehydrogenation of butanes were likely due to the formation of coke on the surface.

ACKNOWLEDGMENTS

Support for this research by the EU (Brite Euram) and the Academy of Finland is gratefully acknowledged. We thank Mr. Leif Backman at Helsinki University of Technology for the TPR work, Ms. Heidi Österholm at Fortum Oil and Gas Oy for the XRD analyses, Mr. Ilkka Savolainen at Fortum Oil and Gas Oy for the XPS measurements, and Ms. Noora Tyynelä at Helsinki University of Technology for measuring the activities of the catalyst samples.

REFERENCES

1. Blasco, T., and López Nieto, J. M., *Appl. Catal. A: Gen.* **157**, 117 (1997).
2. Mamedov, E. A., and Cortés Corberán, V., *Appl. Catal. A: Gen.* **127**, 1 (1995).
3. Cavani, F., and Trifirò, F., *Catal. Today* **51**, 561 (1999).
4. Haber, J., *in* "Handbook of Heterogeneous Catalysis" (G. Ertl, H. Knözinger, and J. Weitkamp, Eds.), Vol. 5, p. 2253, VCH, Weinheim 1997.

5. Pantazidis, A., Bucholz, S. A., Zanthoff, H. W., Schuurman, Y., and Mirodatos, C., *Catal. Today* **40**, 207 (1998).
6. Creaser, D., Andersson, B., Hudgins, R. R., and Silveston, P. L., *J. Catal.* **182**, 264 (1999).
7. Le Bars, J., Auroux, A., Forissier, M., and Vedrine, J. C., *J. Catal.* **162**, 250 (1996).
8. Andersen, P. J., and Kung, H. H., *in* "Studies in Surface Science and Catalysis" (L. Guczi, F. Solymosi, and P. Tétényi, Eds.), Vol. 75, p. 205. Elsevier Science Publishers and Akad. Kiadó, Budapest, 1992.
9. Niemi, V., internal report, Neste 1995.
10. Clark, D. M., Tromp, P. J. J., and Arnoldy, P., U.S. Patent 5 220 092, 1993.
11. Lee, F. M., U.S. Patent 4 607 129, 1986.
12. Lee, F. M., U.S. Patent 4 644 089, 1987.
13. Koranne, M. M., Goodwin, Jr., J. G., and Marcelin, G., *J. Catal.* **148**, 369 (1994).
14. Blasco, T., Galli, A., López Nieto, J. M., and Trifiró, F., *J. Catal.* **169**, 203 (1997).
15. Eberhardt, M. A., Proctor, A., Houalla, M., and Hercules, D. M., *J. Catal.* **160**, 27 (1996).
16. Haber, J., Kozlowska, A., and Kozłowski, R., *J. Catal.* **102**, 52 (1986).
17. Stobbe-Kreemers, A. W., van Leerdam, G. C., Jacobs, J.-P., Brongersma, H. H., and Scholten, J. J. F., *J. Catal.* **152**, 130 (1995).
18. Yoshida, S., Iguchi, T., Ishida, S., and Tarama, K., *Bull. Chem. Soc. Jpn.* **45**, 376 (1972).
19. Wachs, I. E., *Chem. Eng. Sci.* **45**, 2561 (1990).
20. Wachs, I. E., Jehng, J.-M., Deo, G., Weckhuysen, B. M., Guliants, V. V., Benziger, J. B., and Sundaresan, S., *J. Catal.* **170**, 75 (1997).
21. Nag, N. K., Chary, K. V. R., Reddy, B. M., Rao, B. R., and Subrahmanyam, V. S., *Appl. Catal. A: Gen.* **9**, 225 (1984).
22. Hakuli, A., Kytökivi, A., Lakomaa, E.-L., and Krause, A. O. I., *Anal. Chem.* **67**, 1881 (1995).
23. Harlin, M. E., Backman, L. B., Krause, A. O. I., and Jylhä, O. J. T., *J. Catal.* **183**, 300 (1999).
24. Blasco, T., López Nieto, J. M., Dejoz, A., and Vázquez, M. I., *J. Catal.* **157**, 271 (1995).
25. Hakuli, A., Kytökivi, A., Krause, A. O. I., and Suntola, T., *J. Catal.* **161**, 393 (1996).
26. Nag, N. K., and Massoth, F. E., *J. Catal.* **124**, 127 (1990).
27. Eon, J. G., Olier, R., and Volta, J. C., *J. Catal.* **145**, 318 (1994).
28. Chary, K. V. R., and Kishan, G., *J. Phys. Chem.* **99**, 14424 (1995).
29. Oyama, S. T., Middlebrook, A. M., and Somorjai, G. A., *J. Phys. Chem.* **94**, 5029 (1990).
30. Chen, K., Khodakov, A., Yang, J., Bell, A. T., and Iglesia, E., *J. Catal.* **186**, 325 (1999).
31. Resasco, D. E., and Haller, G. L., "Catalysis," Vol. 11, p. 379, Royal Chem. Soc., Cambridge, 1994.